# Effect of Oxygen Environment on Soot Characteristics in Ethylene Laminar Diffusion Flames

**Zeng D.*, Xiong G., Wang Y.**

*FM Global, Research Division, Norwood, MA, 02062, USA*
**Corresponding author's email: dong.zeng@fmglobal.com*

## ABSTRACT

Radiative characteristics and soot distribution of laminar diffusion flame of ethylene is studied experimentally over a wide range of oxygen index (OI) (from 13.3% to 20.9%) and fuel flow rates. The flame is established on a circular burner surrounded by the coflows of various oxygen concentrations. The effect of OI on flame at smoke-point is investigated. When the OI decreases, the smoke-point flame flow rate reduces but the flame length first increases then decreases. The radiant profile along the flame height shows the radiant power shifts to a larger height with increased OI, and the flame radiant fraction reduces. Furthermore, it is found that the radiant fraction of laminar diffusion flame linearly correlates with those of buoyant turbulent flames at the same adiabatic flame temperature. The soot volume fraction of flames of different flow rates under several oxygen concentrations is measured using the laser-induced incandescence (LII) technique. The soot volume fraction distribution shows that the lower OI condition has a smaller soot formation rate. Moreover, as OI reduces, the position for maximum soot volume fraction shifts towards the centerline region at a larger flame height. Compared to the laminar diffusion flames with fuel diluted with nitrogen, the flame with oxidizer diluted has a lower activation energy of 127 kJ/mol of the soot formation reaction.

**KEYWORDS:** Laminar diffusion flame, radiation, soot, laser-induced incandescence.

## INTRODUCTION

In accidental fire and resulting suppression scenarios, fire may occur in vitiated environments due to reduced oxygen by limited air supply, or dilution of oxygen by suppression agents such as water mist or inert gas. The reduced oxygen concentration in the atmosphere (oxygen index, OI) can affect the flame characteristics of buoyant turbulent flames including the flame radiative property by changing the soot volume fraction. A better understanding of the effect of oxygen concentration on the flame characteristics such as the soot volume fraction variation is therefore desirable. In general, flame radiant fraction reduces with a lower oxygen index [1-6]. A recent study of buoyant turbulent ethylene flame [7] shows that the mean soot volume fraction generally reduces with the oxygen index, while the mean soot temperature is similar at different OI, which indicates that the reduction of the radiant fraction is attributed to a lower soot volume fraction. However, due to the transient characteristic of the turbulent flames, the effect of oxygen index on the soot formation and oxidation mechanism is difficult to identify in such conditions.

The effect of reduced reactant concentration on the radiative characteristics of laminar flames has been investigated extensively, including dilution in either fuel [8-15] or oxidizer [16-20]. In general, an inert dilution can 1) reduce flame temperature by the thermal effect, 2) reduce reactants concentration and thus the soot formation rate. For the fuel dilution effect, Axelbaum and Law [8] showed the dilution has a greater effect for soot formation with a moderate dilution level of fuel, but temperature effects may dominate with a larger dilution level of fuel. Gűlder and Snelling [10]

Proceedings of the Ninth International Seminar on Fire and Explosion Hazards (ISFEH9), pp. 107-115
Edited by Snegirev A., Liu N.A., Tamanini F., Bradley D., Molkov V., and Chaumeix N.
Published by St. Petersburg Polytechnic University Press
ISBN: 978-5-7422-6496-5 DOI: 10.18720/spbpu/2/k19-47

demonstrated a similar observation that the effect of dilution on the maximum soot concentration is greater until a dilution fraction of about 0.7, and then smaller with further fuel dilution. For the oxidizer dilution effect, Glassman and Yaccarino [16] showed that the increased oxygen concentration in oxidizer first increases the heat release rate of the smoke-point flame (laminar flame at the fuel flow rate that smoke starts to release from the tip of the flame), then decreases it at higher oxygen concentrations. Such trends are the results of the competing mechanisms of soot formation and oxidation rates. Glassman and Yaccarino also demonstrated that the varying adiabatic flame temperature of oxidizer with different oxygen concentrations is responsible for the variation of soot reaction rate by examining the flames with oxidizer of oxygen and different inert diluents, i.e. $N_2$, Ar. Fuentes et al. [17] showed a consistent observation with Glassman and Yaccarino, and an oxygen index lower than 25% results in a faster decrease of the soot oxidation rate than the formation rate, which results in a lower smoke-point flame heat release rate at lower OI.

While these studies provided the information of how soot formation/oxidation rates vary with the OI, the detailed soot volume fraction of OI lower than that in the normal air is limited. Furthermore, the radiant fraction of the laminar flames at the smoke point of different OI, which has been shown to be important to understand and correlate the radiative characteristics of buoyant turbulent flames [21], was not reported previously. The objective of this work is to study the effect of oxygen index on the radiative properties, especially the radiant fraction and distribution of soot volume fraction, of the laminar diffusion flame. These detailed measurements of laminar diffusion flame will facilitate the understanding and modeling of the buoyant turbulent flames [22, 23].

## EXPERIMENTAL SETUP

The axisymmetric ethylene-air/$N_2$ diffusion flame is established on a Santoro-type laminar flame burner with a circular fuel tube of 16.4 mm I.D., 17.6 mm O.D. The fuel tube is surrounded by an $N_2$-air co-flow passing through a square shape flow straightener of 10×10 $cm^2$, made from two layers of the wire-mesh screen above a layer of 5 cm deep metal beads with 1 mm O.D. The total flow rate of co-flow is maintained at 65 L/min, while the nitrogen to air ratio is adjusted to change OI between 13.3% and 20.9%, which is monitored by a gas analyzer. A mass flow controller (OMEGA FMA5512A) controls the fuel flow rate with a repeatability of ±2.5 $cm^3$/min. The flow rates of air and nitrogen are controlled by two mass flow controllers (Sierra C100L-DD-2-OV1-SV1-PV2-V1-SO and Sierra C100M-DD-3-OV1-SV1-PV2-V1-S0) respectively. The burner and co-flow supply system are placed inside a square shape enclosure with Pyrex panels on the sides and open on the top surface. However, in LII measurements, two side panels are replaced by Thorlabs laser safe barriers with an open slit for the laser sheet to transmit. The burner, co-flow straightener, and enclosure are placed on a translational stage with 0.01mm precision for measurements along the flame height.

The flow rate of smoke-point flame at different OI is determined by visual observation of the appearance/disappearance of smoke in the increasing/decreasing flow rates. The measurement is conducted at least three times, and the average and deviation are then computed. Flame images at the smoke point at different OI are recorded using a Nikon D800 camera, with a Zeiss 135mm F/2 lens with constant exposure time. The radiation measurements of flames at the smoke-point flow rates are conducted using a slit radiometer. The radiometer is equipped with a spectrally flat thermopile sensor (Dexter Research Center, Inc., Model 1M, BaF2 window, and a sensitive area of 1 mm diameter). Shown in Fig. 1, a water-cooled front plate with a horizontal slit opening painted in black restricts the field-of-view of the sensor that it only views a horizontal flame section. The sensor constant and effective height of flame viewed is calibrated using a high-temperature black body. The effective slit height at the flame centerline is 6.87 mm, and the view angle of the slit radiometer is 3º. The slit-radiometer placed on a motorized vertical translation stage traverses flame

height and records the flame radiant power along the flame height, and the total radiant power is calculated by integration of radiative power along the flame length, following the method in reference [7].

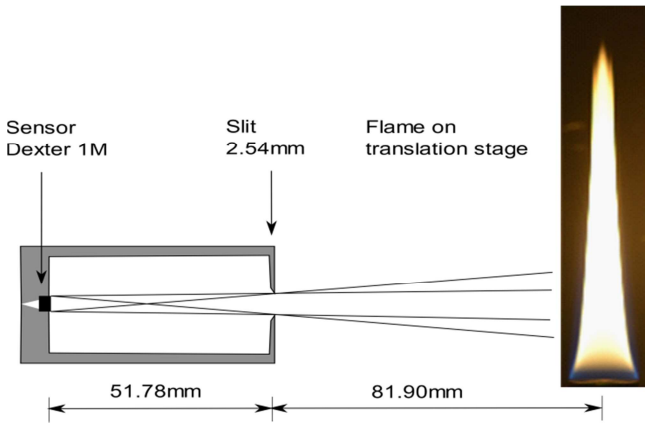


**Fig. 1.** Radiant measurement experimental setup.

The soot volume fraction of flame centerline plane is measured using the laser-induced incandescence (LII) technique as shown in Fig. 2. A dual-cavity Nd:YAG laser (Quantel Twin 850) operates at 10 Hz with 120 mJ/pulse at 532 nm for LII measurements. The laser sheet is formed using a 1000 mm focal-length spherical lens and a -150 mm focal-length cylindrical lens. The LII signal is collected with a Nikon AF Nikkor lens (50 mm focal length with f/2) to an intensified sCMOS (scientific-complementary metal-oxide-semiconductor) camera (Andor iStar sCMOS 18F-64). A bandpass filter centered at 425 nm (with a full-width half max (FWHM) of 50 nm and an optical-density of 4) is used before the lens to eliminate interferences from the $C_2$ swan band emission. The prompt LII with no gate delay from laser pulse arrival is employed for signal detection to minimize the bias for quantitative measurement [24]. Table 1 shows the experimental conditions of LII measurement.

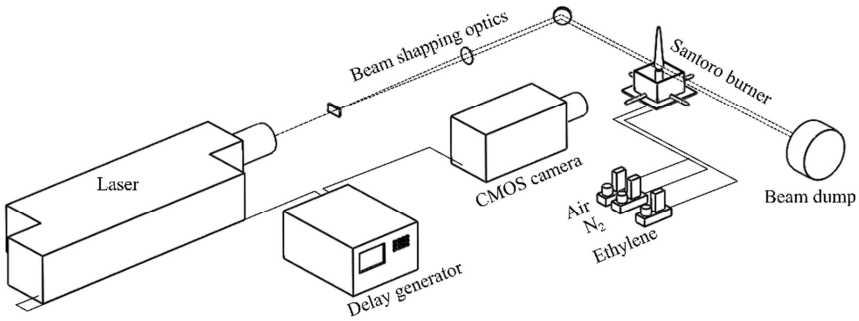


**Fig. 2.** LII experimental setup for laminar flame soot measurement.

**Table 1. LII experimental parameters and constant**

| OI (%) | Fuel flow | Coflow | |
|---|---|---|---|
| | $C_2H_4$ ($cm^3/s$) | Air (L/min) | $N_2$ (L/min) |
| 20.9 | 3.85, 3.25, 2.8, 2.53 | 65 | 0 |
| 16.8 | 3.25, 2.8, 2.53 | 52.5 | 12.5 |
| 15.2 | 2.8, 2.53 | 47.5 | 17.5 |

## RESULT AND DISCUSSION

### Smoke point flame radiation

Figure 3 shows images of the smoke-point ethylene flame in co-flows with different OI. When the OI reduces from 20.9% (normal air), the smoke-point flame height increases slightly at 19.4% $O_2$ but then decreases with the further lower oxygen concentration. With a lower OI, the flame luminosity generally reduces, with a relatively more significant reduction near the flame bottom. The smoke point flame morphology differs among different OI. In the normal air condition, the smoke point flame shows the wing-like soot layer near the flame tip. However, such a wing-like soot layer is not observed at OI below 18%. Instead, smoke is released from the flame tip when the flame is above the smoke point. This morphology change will be discussed further with the soot volume fraction distribution in the following context.

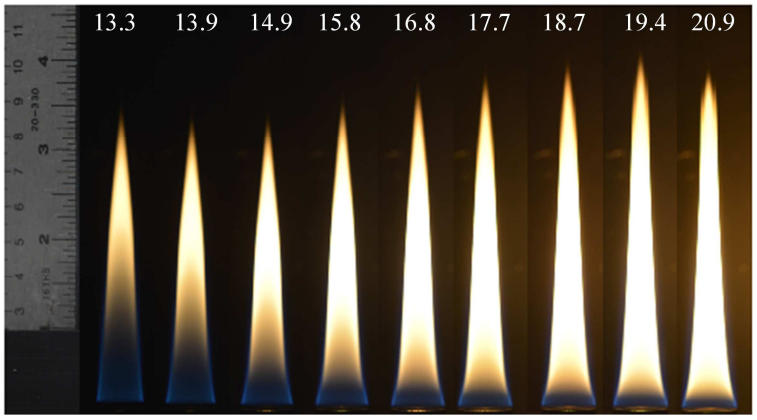


**Fig. 3.** Laminar ethylene flames at smoke point in different OI.

Figure 4(a) shows the smoke-point flow rate at a wide range of OI from 13.3% to 20.9%. These results are in good agreement with available data at OI of 16% to 22% from Glassman and Yaccarino [16]. The increased standard deviation at lower OI, such as 14% $O_2$, is a result of the lower soot concentration and the corresponding smaller amount of smoke released from the flame tip near the smoke point, which is more challenging to observe. The lower smoke-point flow rate with the lower OI has been attributed to a faster reducing of soot oxidation rate than soot formation rate as OI reduces in the range of 24% and 16% [16]. Nonetheless, the smoke-point flame flow rate changes less at OI lower than 14.5%, indicating a similar reduction in soot formation rate and oxidation rate. Figure 4(b) shows the radiant power distribution along the flame height of the laminar smoke-point flames with the different OI. The radiant power increases along the flame axis and reaches the maximum value at a height above the burner (HAB) of 3~5 cm. The location for the peak radiant power shifts slightly to a higher HAB as OI reduces. Overall, the radiant power reduces at lower OI because of the lower soot concentration and adiabatic flame temperature, as shown in Fig. 4(c).

The radiative properties of the laminar flames are important for the understanding and prediction of properties of the turbulent flames. Markstein [21] showed that the radiant fraction of buoyant turbulent flame could be correlated with the laminar smoke point flame height for several hydrocarbon fuels with similar adiabatic flame temperatures, such as ethylene, ethane, propylene, and propane, Markstein found that the total heat loss fraction (radiant and burner loss) of laminar flame is approximately 0.30 at the smoke point. Orloff at al. [3] confirmed that the smoke point is

the principal chemical variable controlling turbulent buoyant flame radiation, but they also showed that the radiant fraction depends on the adiabatic flame temperature as well.

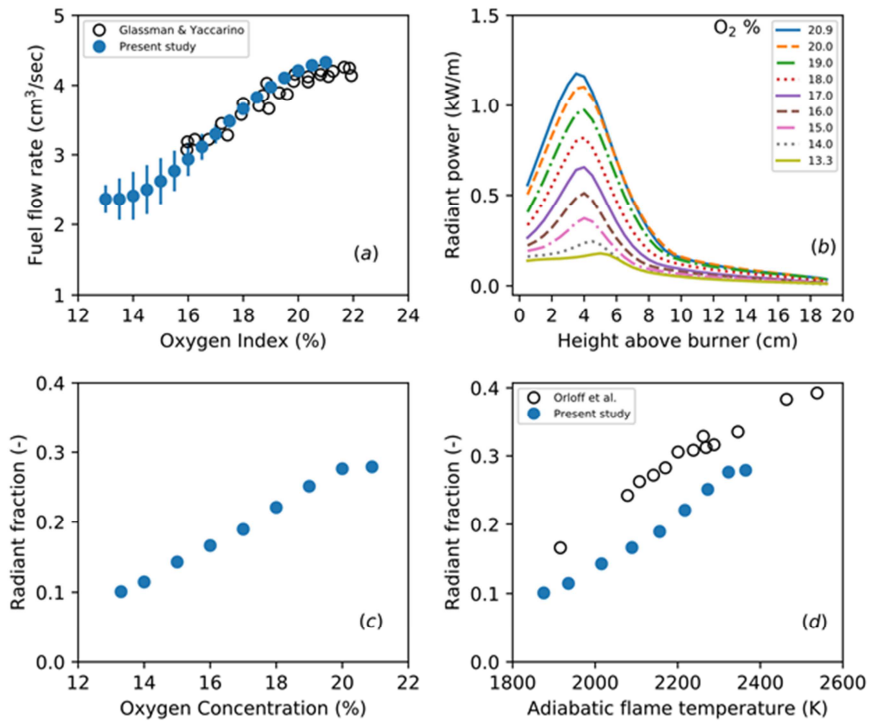


**Fig. 4.** Laminar ethylene flames characteristics in different OI, (a) smoke-point flow rate; (b) radiant power distribution of the smoke point flame at different OI, (c) radiant fraction of the smoke-point flame at different OI, (d) correlation of radiant fractions of laminar smoke-point flames and turbulent flames at different OI.

In the current study, the oxygen concentration in the oxidizer is varied which results in the different adiabatic flame temperatures. Therefore, Markstein's correlation is not valid for the conditions studied. Orloff at al. [3] measured the radiant fraction of buoyant turbulent ethylene flames with different oxidizer dilution. When the smoke-point radiant fraction for laminar flame and buoyant turbulent flame are plotted versus the adiabatic flame temperature, shown in Fig. 4(d), a similar dependence of the radiant fraction on adiabatic flame temperature, or OI, exists for both laminar and buoyant turbulent flames of ethylene fuel. Such a similarity indicates that radiant fraction of a smoke-point laminar flame is related to those of a buoyant turbulent flame at the same OI. In a reduced oxygen concentration environment, the smaller soot concentration of a laminar smoke-point flame is mainly responsible for its reduced radiant fraction. The similarity in Fig. 4(d) shows such a soot concentration reduction may also be mainly responsible for the corresponding reduction of the radiant fraction in a buoyant turbulent flame [7]. Such similarity between laminar and turbulent flames could potentially be established for different fuels, which is a future work.

**Soot volume fraction measurement**

Soot volume fraction $f_v$ is measured with LII to provide more detailed information for the understanding of soot formation and oxidation at different OI. The LII measurement is calibrated by comparing the LII signals to the laser extinction measurements of a laminar diffusion flame [25]. The calibration constant can be obtained from

$$C = -\frac{\lambda}{K_e}\ln(I/I_0)\left(\int_0^L S_{LII}\,dx\right)^{-1}, \tag{1}$$

where λ is the wavelength of the laser used in the extinction measurement, $I$ and $I_0$ are the laser intensities after and before extinction, $L$ is the flame pathlenth, $S_{LII}$ is the spatially varying LII signal, and $K_e$ is the extinction coefficient which is independent of particle size

$$K_e = 6\pi\,\mathrm{Im}\left(\frac{m_\lambda^2-1}{m_\lambda^2+2}\right) = \frac{36\pi n_\lambda k_\lambda}{\left(n_\lambda^2-k_\lambda^2+2\right)^2+\left(2n_\lambda k_\lambda\right)^2}, \tag{2}$$

where $n_\lambda$ and $k_\lambda$ are the real and imaginary part of the complex refractive index $m_\lambda$ (i.e., $m_\lambda = n_\lambda + i\,k_\lambda$) of soot evaluated at the laser wavelength. The refractive index is available from the studies of Dalzell and Sarofim [26], Lee and Tien [27], or Chang and Charalampopoulos [28]. It is worth noting that calibration constant and thus the measured soot volume fraction is dependent on the selection of refractive index. In the current study, the optical constants of Dalzell and Sarofim are selected, which is $m_\lambda = 1.583 - 0.568i$ at the 633 $nm$ wavelength used in the extinction experiment. The comparison between current measurement and the result from Quay et al. [29] shows a good consistency at the same ethylene flow rate of 3.85 cm$^3$/sec and OI of 20.9%, as shown in Fig. 5. The difference may be attributed to the different burner geometry, e.g. the current burner has a I.D of 16.4 mm, larger than Quay et al.'s burner with a 11.1 mm I.D.

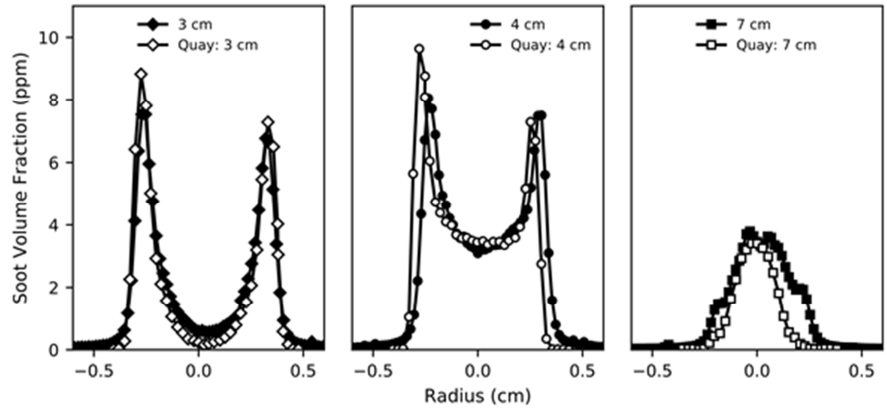


**Fig. 5.** Comparison of radial distributions of the soot volume fraction measurement with Quay et al. [29], ethylene fuel flow rate is 3.85 cm$^3$/sec, OI is 20.9%.

## EFFECT OF OXYGEN INDEX ON SOOT VOLUME FRACTION DISTRIBUTION

Figure 6 shows the soot volume fraction distribution of the centerline plane of ethylene flame with a same fuel flow rate of 2.8 cm$^3$/s but different OI (20.9, 16.8, and 15.2%). In the normal air, soot $f_v$ reaches nearly 7 ppm at 4 cm HAB, then decreases due to increased oxidation. With a reduced OI, soot $f_v$ reduces to 3 and 1 ppm at 4 cm HAB in 16.8 and 15.2% $O_2$ respectively, which indicates a reduced soot formation rate at lower OI. This reduced soot formation rate can be attributed to the reduced adiabatic flame temperature. The maximum soot $f_v$ of 16.8 and 15.2% $O_2$ are achieved at flame heights of 5 and 7 cm respectively. This shift of peak-soot location towards a higher HAB implies a faster decrease of the soot oxidation rate than the formation rate, which is consistent with results from Fuentes et al. [17]. Furthermore, the soot volume fraction distribution changes as OI

reduces. At lower OI, the maximum soot $f_v$ occurs in the centerline region of flame instead of on the edge of flame in the normal air condition, which results in the disappearance of the wing-like structure in low OI conditions shown in Fig. 3.

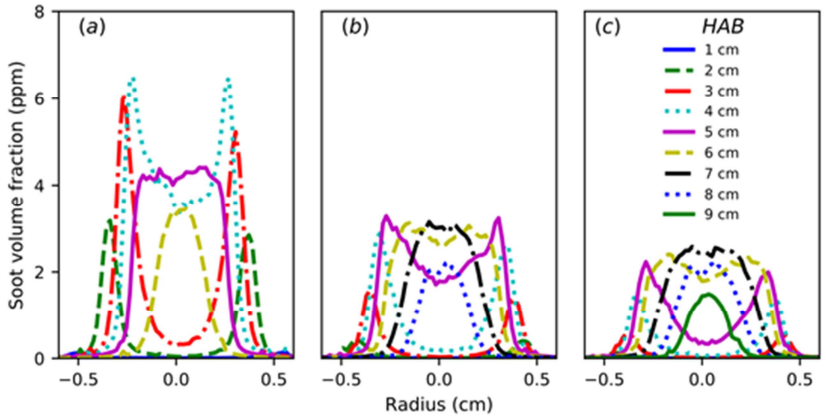


**Fig. 6.** Radial distributions of soot volume fraction, 2.8 $cm^3$/sec, (a) normal air; (b) 16.8% $O_2$; (c) 15.2% $O_2$.

Figure 7 compares the average soot $f_v$ of with height at different OI and flow rates using [14]

$$f_{v,z} = \frac{1}{\pi r_f^2}\int_0^{r_f} 2\pi r_f f_v(r,z)\,dr\,, \tag{3}$$

where $r_f$ is the flame radius at different height, $f_v(r,z)$ is the soot $f_v$ at different radius and height. For each OI condition, the increase of fuel flow rate does not significantly vary the maximum average soot $f_v$ but elevates the location of maximum $f_v$. This can be explained by the reaction time needed for soot formation, therefore longer distance to reach peak soot volume fraction for lower flow rate conditions. The maximum average soot $f_v$ decrerases as OI changes from 20.9% to 15.2%. The lower soot $f_v$, along with the reduced adiabatic flame temperature, results in a lower radiant power from flame, as shown in Fig. 4.

## INHIBITION OF SOOT FORMATION BY NITROGEN DILUTION

Nitrogen dilution in either fuel or oxidizer can both reduce the soot formation rate. Compared to the dilution effect for oxidizer, the fuel dilution reduces soot formation by reducing both the adiabatic flame temperature and the fuel reactant concentration. To compare the soot formation inhibition effect of nitrogen dilution in fuel or oxidizer, we follow the approach of Gülder and Snelling [10] by expressing the soot formation rate as

$$\dot{m}'_{soot} \propto [X_F]^a \frac{\sqrt{H}}{L_{max}} \exp\left(-\frac{E_a}{RT}\right), \tag{4}$$

where $X_F$ is the fuel fraction in the diluted fuel, $H$ is the flame height and $L_{max}$ is the flame diameter at the axial location of the maximum soot volume fraction, $E_a$ is the soot formation activation energy ($J/mol$), $R$ is the ideal gas constant (8.314 $J/mol \cdot K$), and $T$ is temperature ($K$). The effect of flame geometry variation due to dilution is reflected in the term $\sqrt{H}/L_{max}$. It was assumed that the soot formation along the flame axis is independent from the soot oxidation, except in the flame tip region. Using the adiabatic flame temperature and soot volume fraction data from Fig. 7, Eq. (4) yields an activation energy of 127 kJ/mol, smaller than an activation energy of 200

kJ/mol of the soot formation rate based on the data from the laminar diffusion flames with fuel diluted with nitrogen [8, 10, 13]. Such a difference seems to indicate the soot inhibition effect is smaller when oxidizer is diluted than that the fuel is diluted to a same adiabatic flame temperature. The mechanism for such a difference should be further studied.

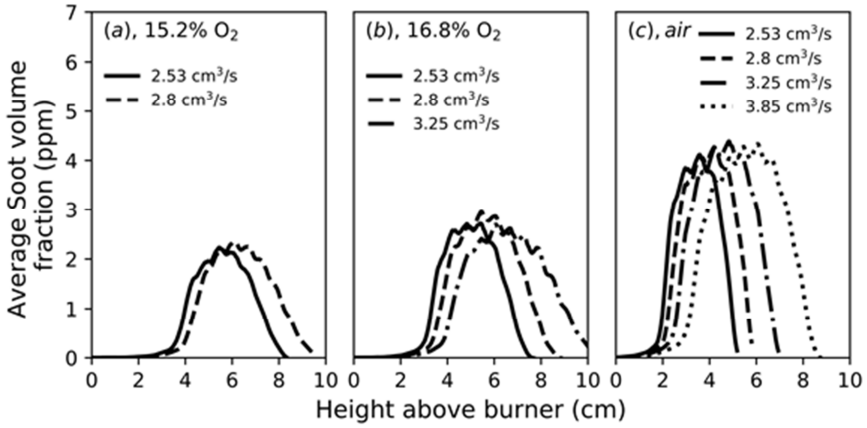


**Fig. 7.** Comparison of average soot volume fraction profiles of different OI and fuel flow rates.

## CONCLUSIONS

This study investigates the effect of oxygen index on the smoke point flame characteristics and soot volume fraction distribution, and the detailed soot volume fraction distribution of laminar diffusion flames of different OI and fuel flow rates. The smoke-point flame flow rate reduces but the flame length first increases then decreases with decreased OI. The radiant power profile along the flame axis shifts to a higher height at lower OI and the flame radiant fraction reduces. Such variations are consistent with the soot volume fraction distribution at different OI. At lower OI, the flame has a smaller soot formation rate and lower maximum soot volume fraction that occurs at a larger flame height. Also, the radiant fraction of laminar ethylene diffusion flame linearly correlates with those of buoyant turbulent ethylene flames at the same adiabatic flame temperature. Compared to the laminar diffusion flame with fuel dilution with nitrogen, the global activation energy of soot formation reaction in oxidizer diluted laminar diffusion flame is lower at 127 kJ/mol, indicating lower soot inhibition effect for the oxidizer dilution compared to fuel dilution condition. This study extends the smoke point measurement into the lower OI and provides the detailed soot volume fraction data which will be applied to improve the smoke-point based radiation model.

## REFERENCE

[1] G. Santo, F. Tamanini, Influence of oxygen depletion on the radiative properties of PMMA flames, Proc. Combust. Inst. 18 (1981) 619-631.

[2] G. Santo, M.A. Delichatsios, Effects of vitiated air on radiation and completeness of combustion in propane pool fires, Fire Saf. J. 7 (1984) 159-164.

[3] L. Orloff, J. de Ris, M.A. Delichatsios, Radiation from buoyant turbulent diffusion flames, Combust. Sci. Technol. 84 (1992) 177-186.

[4] A. Tewarson, J.L. Lee, R.F. Pion, The influence of oxygen concentration on fuel parameters for fire modeling, Proc. Combust. Inst. 18 (1981) 563-570.

[5] A. Nasr, S. Suard, H. El-Rabii, J.P. Garo, L. Gay, L. Rigollet, Heat feedback to the fuel surface of a pool fire in an enclosure, Fire Saf. J. 60 (2013) 56-63.

[6] J.P. White, E.D. Link, A.C. Trouvé, P.B. Sunderland, A.W. Marshall, J.A. Sheffel, M.L. Corn, M.B. Colket, M. Chaos, H.Z. Yu, Radiative emissions measurements from a buoyant, turbulent line flame under oxidizer-dilution quenching conditions, Fire Saf. J. 76 (2015) 74-84.
[7] D. Zeng, P. Chatterjee, Y. Wang, The effect of oxygen depletion on soot and thermal radiation in buoyant turbulent diffusion flames, Proc. Combust. Inst. (2018).
[8] R.L. Axelbaum, C.K. Law, Soot formation and inert addition in diffusion flames, Proc. Combust. Inst. 23 (1991) 1517-1523.
[9] K.P. Schug, Y. Manheimer-Timnat, P. Yaccarino, I. Glassman, Sooting Behavior of Gaseous Hydrocarbon Diffusion Flames and the Influence of Additives, Combust. Sci. Technol. 22 (1980) 235-250.
[10] Ö.L. Gülder, D.R. Snelling, Influence of nitrogen dilution and flame temperature on soot formation in diffusion flames, Combust. Flame 92 (1993) 115-124.
[11] C.S. McEnally, L.D. Pfefferle, The Effect of Nitrogen Dilution on Nonfuel Hydrocarbons in Laminar Nonpremixed Flames, Combust. Sci. Technol. 151 (2000) 133-155.
[12] F. Liu, H. Guo, G.J. Smallwood, Ö.L. Gülder, The chemical effects of carbon dioxide as an additive in an ethylene diffusion flame: implications for soot and NOx formation, Combust. Flame 125 (2001) 778-787.
[13] Q. Wang, G. Legros, J. Bonnety, C. Morin, Experimental characterization of the different nitrogen dilution effects on soot formation in ethylene diffusion flames, Proc. Combust. Inst. 36 (2017) 3227-3235.
[14] Q. Wang, G. Legros, J. Bonnety, C. Morin, A. Matynia, J.-L. Consalvi, F. Liu, Experimental assessment of the sudden-reversal of the oxygen dilution effect on soot production in coflow ethylene flames, Combust. Flame 183 (2017) 242-252.
[15] R.K. Abhinavam Kailasanathan, T.L.B. Yelverton, T. Fang, W.L. Roberts, Effect of diluents on soot precursor formation and temperature in ethylene laminar diffusion flames, Combust. Flame 160 (2013) 656-670.
[16] I. Glassman, P. Yaccarino, The effect of oxygen concentration on sooting diffusion flames, Combust. Sci. Technol. 24 (1980) 107-114.
[17] A. Fuentes, R. Henríquez, F. Nmira, F. Liu, J.-L. Consalvi, Experimental and numerical study of the effects of the oxygen index on the radiation characteristics of laminar coflow diffusion flames, Combust. Flame 160 (2013) 786-795.
[18] I.S. McLintock, The effect of various diluents on soot production in laminar ethylene diffusion flames, Combust. Flame 12 (1968) 217-225.
[19] F. Escudero, A. Fuentes, J.L. Consalvi, F. Liu, R. Demarco, Unified behavior of soot production and radiative heat transfer in ethylene, propane and butane axisymmetric laminar diffusion flames at different oxygen indices, Fuel 183 (2016) 668-679.
[20] F. Escudero, A. Fuentes, R. Demarco, J.L. Consalvi, F. Liu, J.C. Elicer-Cortés, C. Fernandez-Pello, Effects of oxygen index on soot production and temperature in an ethylene inverse diffusion flame, Exp. Thermal Fluid Sci. 73 (2016) 101-108.
[21] G.H. Markstein, Relationship between smoke point and radiant emission from buoyant turbulent and laminar diffusion flames, Proc. Combust. Inst. 20 (1985) 1055-1061.
[22] P. Chatterjee, J.L. de Ris, Y. Wang, and S.B. Dorofeev, A model for soot radiation in buoyant diffusion flames, Proc. Combust. Inst. 33 (2011) 2665-2671.
[23] P. Chatterjee, Y. Wang, K.V. Meredith, and S.B. Dorofeev, Application of a subgrid soot-radiation model in the numerical simulation of a heptane pool fire, Proc. Combust. Inst. 35 (2015) 2573-2580.
[24] R.L. Vander Wal, Laser-induced incandescence: detection issues, Appl. Opt. 35 (1996) 6548-6559.
[25] C.R. Shaddix, K.C. Smyth, Laser-induced incandescence measurements of soot production in steady and flickering methane, propane, and ethylene diffusion flames, Combust. Flame 107 (1996) 418-452.
[26] W.H. Dalzell, A.F. Sarofim, Optical constants of soot and their application to heat-flux calculations, J. Heat Transfer 91 (1969) 100-104.
[27] S.C. Lee, C.L. Tien, Optical constants of soot in hydrocarbon flames, Proc. Combust. Inst. 18 (1981) 1159-1166.
[28] H. Chang, T.T. Charalampopoulos, Determination of the Wavelength Dependence of Refractive Indices of Flame Soot, Proc. R. Soc. Lond. A 430 (1990) 577-591.
[29] B. Quay, T.W. Lee, T. Ni, and R.J. Santoro, Spatially resolved measurements of soot volume fraction using laser-induced incandescence, Combust. Flame 97 (1994) 384-392.